COSY Beam Time Request

For Lab. use	
Exp. No.:	Session No.
E 005.7	**12**

Collaboration: **JEDI**

First electric dipole moment measurement of the deuteron with the waveguide RF Wien Filter (2nd run)

Jülich, 08.09.2020

Spokespersons for the beam time:
Frank Rathmann (Jülich)
Alexander Nass (Jülich)
Giuseppe Tagliente (INFN, Bari, Italy)

Spokespersons for the collaboration:
Paolo Lenisa (Ferrara)
Jörg Pretz (Aachen/Jülich)

Address:
Institut für Kernphysik
Forschungszentrum Jülich
52428 Jülich
Germany

Phone: **+49 2461 61 4558** Fax: **+49 2461 61 3930**

E-mail:
f.rathmann@fz-juelich.de
a.nass@fz-juelich.de
giuseppe.tagliente@ba.infn.it

lenisa@fe.infn.it
pretz@physik.rwth-aachen.de

Total number of particles and type of beam (p, d, polarization)	Kinetic energy (MeV)	Intensity or internal reaction rate (particles per second) minimum needed	Intensity or internal reaction rate (particles per second) maximum useful
Polarized deuterons	**~970 MeV/c**	**stored ~10^9**	**stored ~10^{10}**
Experimental area	Safety aspects (if any)	Earliest date of installation	Total beam time (No. of shifts)
JEPO detector, RF Wien filter, electron cooler, RF solenoid, Siberian snake	**none**	**January 15, 2020**	**2 MD + 5 weeks**

First electric dipole moment measurement of the deuteron with the waveguide RF Wien Filter

Proposal for the 2^{nd} run

Achim Andres[1], Volker Hejny[2], Vsevolod Kamerdzhiev[2], Paolo Lenisa[3], Alexander Nass[2], Jörg Pretz[2,1], Frank Rathmann[2], Giuseppe Tagliente[4], Vera Shmakova[2], and Jamal Slim[1]

[1]III. Physikalisches Institut B, RWTH Aachen University, 52056 Aachen, Germany
[2]Institut für Kernphysik, Forschungszentrum Jülich, 52428 Jülich, Germany
[3]University of Ferrara and INFN, 44100 Ferrara, Italy
[4]INFN, 70125 Bari, Italy

for the JEDI collaboration*

September 8, 2020

Abstract

The JEDI collaboration would like to request beam time for a 2^{nd} run to measure for the first time the deuteron electric dipole moment at COSY. The preliminary results from the 1^{st} run and from the commissioning effort that took place since then with the aim to improve the machine and the experimental setup are presented.

For the 2^{nd} run of the first deuteron EDM measurement with the RF Wien filter set up without ferrites, **we would like to request 2 weeks of machine development time and 5 weeks of measurement time**, to be tentatively scheduled at the end of the 1^{st} quarter 2021. It should be noted that we would like to combine the beam time for this 2^{nd} precursor run (E 005.7) with the beam time requested for the JEPO commissioning experiment (E 002.8).

*http://collaborations.fz-juelich.de/ikp/jedi/index.shtml

Contents

1 Introduction

A permanent electric dipole moment (EDM) of a particle or a system of particles is a separation of charge along its angular momentum axis and is considered a direct signal of T violation, and, assuming CPT symmetry to hold, also of CP violation. For more than 60 years EDMs have been studied, first as a signal of a parity-symmetry violation and then as a signal of CP violation that would clarify its role in nature and in theory. Contemporary motivations include the role that CP violation plays in explaining the cosmological matter-antimatter asymmetry and the search for physics beyond the Standard Model (BSM) (for review articles, see *e.g.*, Refs. [1, 2]).

The principle idea to search for EDMs of deuterons and protons in a magnetic machine where the sensitivity is clearly lower than in a dedicated EDM machine, is primarily motivated by the need to learn how best to carry out such experiments, and to perfect the experimental methods and techniques. Using an RF Wien filter, it has been shown that the EDM induced spin rotations can be *accumulated* when the Wien filter is operated in phase with the spin precession of the stored particles (see Refs. [3, 4, 5]). The search for the deuteron EDM, presently being pursued by the JEDI collaboration, is one of the main objectives of an Advanced Grant of the European Research Council, awarded in 2015 [6]. During the previous evaluation of the Helmholtz-Gemeinschaft, the part of the research program at Jülich related to the EDM search at COSY has been rated "outstanding".

Besides the pursuit of charged particle EDM experiments at COSY and the further development of the related key technologies, the group is presently also working on the preparation of the next steps that shall lead the way toward a dedicated ultimate-precision EDM storage ring. Recently, together with experts from CERN and JEDI, the CPEDM collaboration has been established[1]. A detailed feasibility study that shall be published as a CERN Yellow Report in the near future is in preparation (see Ref. [7]). As major next step, the design, building and operation of a Prototype Ring (PTR) is considered, that shall be operated to answer the remaining open questions (see Chapters 5 and 7 of Ref. [7]).

The results of the 1$^{\text{st}}$ deuteron EDM run at COSY are discussed in Sec. 2.1, in Sec. 2.2 the approach using a pilot bunch is described that we would like to pursue in the 2$^{\text{nd}}$ run, and a brief summary of the primary goals of the 2$^{\text{nd}}$ run is given in Sec. 2.3. In Sec. 3, a detailed account of the various technical improvements of COSY and of the RF Wien filter is given. Various other aspect are briefly summarized in Sec. 3.4. The request for beam time is presented in Sec. 4.

2 Results from the 1$^{\text{st}}$ deuteron EDM run

Although obvious from the very beginning, EDM related experiments are intrinsically complicated and very difficult to perform. The CBAC granted for the 1$^{\text{st}}$ deuteron EDM run two weeks for machine development and four weeks of actual beam time. Perfecting all involved techniques constituted the primary objective and this again proved very time consuming. Setting up the machine, including the adjustment of all relevant beam parameters, orbit corrections, target setup, detector operations, Wien filter setup and tuning, and the chromaticity adjustments and measurements to ensure a long spin-coherence time, took most of the allocated time. To put this into perspective, eventually we were able to run for about 6 days with the desired machine conditions during the 1$^{\text{st}}$ EDM precursor run. It should be emphasized that the 1$^{\text{st}}$ run carried out in the fall of 2018

[1] http://pbc.web.cern.ch/edm/edm-default.htm

provided necessary input and reconfirmed the need for an ambitious improvement process that was started in parallel to the challenging EDM experiments at COSY. Some of the highlights of the ongoing optimization activities and recent, excellent achievements of young investigators are described in some detail in Sec. 3.

2.1 Preliminary results

According to the generalized Thomas-BMT equation [8], in the presence of an EDM, the invariant spin axis in an ideal ring would be tilted in radial direction. In reality, however, there are additional magnetic misalignments, so that the invariant spin axis is tilted in both radial and longitudinal directions. The goal achieved during the 1st precursor run was to determine the tilt of the invariant spin axis which allows us to obtain an experimental access to the EDM. The determination of the EDM then amounts to an accurate spin dynamics calculation using the magnetic imperfections of the machine, and the difference to the measured result, yields the EDM.

In order to induce a vertical polarization build-up, the RF Wien filter [5, 9] was operated on a harmonics of the spin precession frequency ($\approx 871\,\mathrm{kHz}$), and the RF phase was locked with the spin-precession phase. In this case, a particle passing through the RF Wien filter gets a spin kick in the same direction every turn. In order to obtain a map of the EDM resonance strength, the measurements were performed for different RF Wien filter rotations around the beam axis and for different settings of a solenoid in the opposite straight section which rotates the invariant spin axis at the RF Wien filter longitudinally. 31 points in total were measured during the 1st precursor run in November - December 2018. The initial slopes of the polarization build-up ($\dot{\alpha}$) were observed for various phases of the RF Wien filter, resulting in the sinusoidal dependencies. The map of all data points for the measured $\dot{\alpha}$, interpreted as EDM resonance strength $\varepsilon^{\mathrm{EDM}}$ of deuterons with momenta of 970 MeV/c depending on the RF Wien filter rotation angles and solenoid settings is shown in Fig.1. An analytic expression for the function describing the surface is derived in Eq. (A5) of Ref. [5]. The fit function reads

$$\varepsilon^{\mathrm{EDM}} = \frac{\chi_{\mathrm{WF}}}{4\pi}\left[A_{\mathrm{WF}}^2(\phi^{\mathrm{WF}} - \phi_0^{\mathrm{WF}})^2 + A_{\mathrm{Sol}}^2(\xi_0^{\mathrm{Sol}} + \frac{1}{2\sin\pi\nu_s}\xi^{\mathrm{Sol}})^2\right]^{\frac{1}{2}} + e_0\,, \tag{1}$$

it represents a square root of an elliptic paraboloid, which means there appear quadratic dependencies of the $\varepsilon^{\mathrm{EDM}}$ for both the RF Wien filter rotations and the solenoid settings. Here χ_{WF} is a rotation angle in the Wien filter, ϕ^{WF} and ξ^{Sol} are Wien filter and solenoid setting respectively. The minimum of the surface, given by

$$\begin{aligned} \phi_0^{\mathrm{WF}} &= -3.80 \pm 0.05\,\mathrm{mrad}\,, \\ -\xi_0^{\mathrm{Sol}} &= -5.68 \pm 0.05\,\mathrm{mrad}\,. \end{aligned} \tag{2}$$

corresponds to the orientation of the invariant spin axis at the location of the RF Wien filter. The scaling coefficients amount to

$$\begin{aligned} A_{\mathrm{WF}} &= 0.57 \pm 0.005\,, \\ A_{\mathrm{Sol}} &= 0.84 \pm 0.008\,, \text{ and the offset} \\ e_0 &= (-1.1 \pm 0.1) \times 10^{-10}\,. \end{aligned} \tag{3}$$

The reduced χ^2/ndf of the fit to the data of Fig. 1 using the fit function given in Eq. (1) amounts to

$$\chi^2/\mathrm{ndf} = 459/26 = 17.65\,. \tag{4}$$

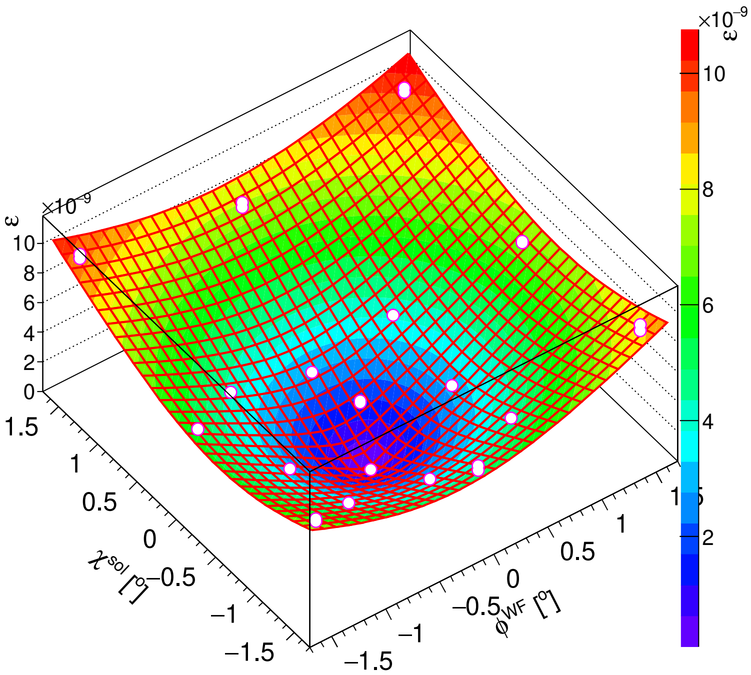

Figure 1: Preliminary experimentally observed parametric resonance strength $\varepsilon \simeq \dot{\alpha}/\omega_{\rm rev}$, plotted in terms of the initial slope $\dot{\alpha}_{|t=0}$, for various values of $\phi_0^{\rm WF}$ and $\chi_0^{\rm sol}$. The surface is a fit to the data using the analytic expression of Eq. (1). The minimum of this graph yields the orientation of the invariant spin axis, the parameters are given in Eq. (2).

2.2 Improved spin-tune feedback using a pilot bunch

During the EDM measurement using the RF Wien filter one would like to ensure that the Wien filter is operated on resonance with the spin-precession frequency of the stored deuterons in the machine. The spin tune is actually defined only for a *static* machine, *i.e.*, for a machine where no RF device is affecting the polarization evolution of the beam. In case, there is a time-dependent *running* or *instantaneous* spin tune, the direction of the invariant spin axis $\vec{n}_s$ also changes as a function of time, i.e., $\vec{n}_s \equiv \vec{n}_s(t)$ (see Ref. [5]).

Thus, operating the RF Wien filter actually modifies the spin tune in the machine, as shown in Fig. 2, and this is unavoidable. What can be avoided, however, is the use of the running spin tune to provide the input to the spin-tune feedback system. Instead, we came up with a new scheme, where multiple bunches (typically four) are stored in the machine, and only three of these bunches are used to determine the EDM resonance strengths, while the fourth one, not affected by the RF Wien filter, is used to determine the spin tune as if the machine were static. The latter can be accomplished by implementing a set of four fast RF switches into the input ports to the RF Wien filter (for technical details, see Sec. 3.3.2).

In this context, it should be emphasized that the pilot-bunch technique provides a co-magnetometer, because it allows us to monitor changes of the experimental setup of the machine with all its imperfections *during* the EDM measurement, like, e.g., drifts of the magnetic field.

The pilot bunch concept is presently being tested experimentally with beam during the ongoing JEDI beam time (see JEDI proposal E005.6 [10]). Results obtained shall be

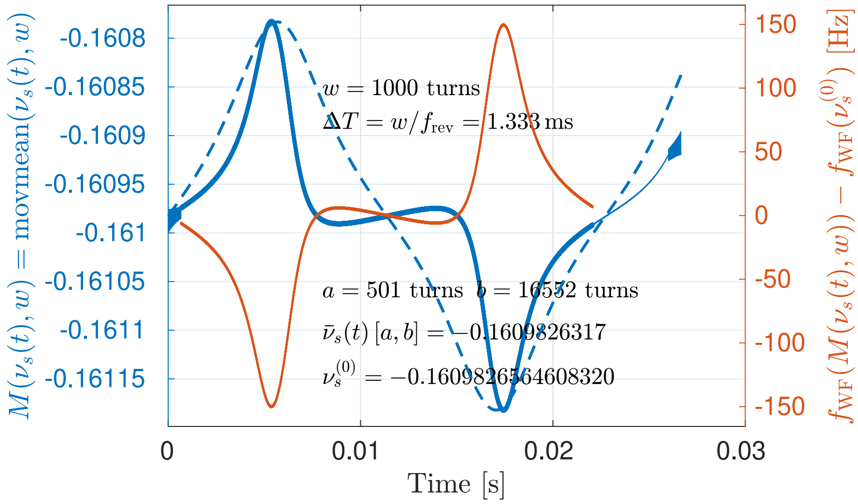

Figure 2: Simulated data for the running spin tune of deuterons stored in COSY at the nominal JEDI conditions, using an RF Wien filter in EDM mode with a field amplification factor of 10^3, operating exactly at the spin precession frequency. Left scale: Moving mean of the spin tune $M(\nu_s(t), w)$. The dashed line is an analytic prediction of the time dependence of the running spin tune $\nu_s(t)$. Right scale: Corresponding running frequency difference $\Delta f_{\mathrm{WF}}(\nu_s(t))$.

presented at the upcoming CBAC meeting.

A potential new application of the pilot bunch approach JEDI is pursuing, is that one could selectively gate an RF system in a way that individual stored particle bunches are not exposed to the RF. Thereby, the spin manipulation of the particles of a specific bunch stored in a machine may become possible.

2.3 Goals for the 2$^{\text{nd}}$ run

The map of EDM resonance strengths $\varepsilon^{\mathrm{EDM}}$, determined from the initial slopes of the polarization buildup and shown in Fig. 1, is not completely understood. From the theoretical point of view, the fitted parameters A_{WF} and A_{Sol}, given in Eq. (3), should both be equal to unity (see Eq. (A5) of Ref. [5]). In addition, the χ^2/ndf is not good, which indicates that there are not yet understood systematic effects present. In order to improve this situation, we would like to apply a different technique for the determination of the EDM resonance strength during the 2$^{\text{nd}}$ run. The present spin-tune feedback system has another drawback in that it does not allow one to accumulate the polarization build-up beyond the first maximum of the vertical spin component. Using the pilot bunch approach, discussed above, we should be able to determine the unperturbed spin tune in the machine during cycles that extend for as long as the spin-coherence time permits. Thus, we shall be able to stay on resonance for the duration of the full cycle time.

2.3.1 Determination of $\varepsilon^{\mathrm{EDM}}$ based on the oscillation frequency of $p_y(t)$

With the pilot bunch spin-tune feedback in place, the oscillation of the vertical polarization component p_y is expected to proceed as depicted in Fig. 3. These data were obtained from simulations, described in Ref. [5]. The upper panel shows the initial slope $\dot{p}_y|_{t=0}$ as function of the RF phase ϕ^{RF}. The middle panel shows the oscillation frequency ω of p_y also as function of the RF phase ϕ^{RF}. Obviously, ω is independent of ϕ^{RF}, and the phases should just be properly fixed, so that the frequencies can be determined with small errors. As a consequence, the number of build-up measurements at different RF phases

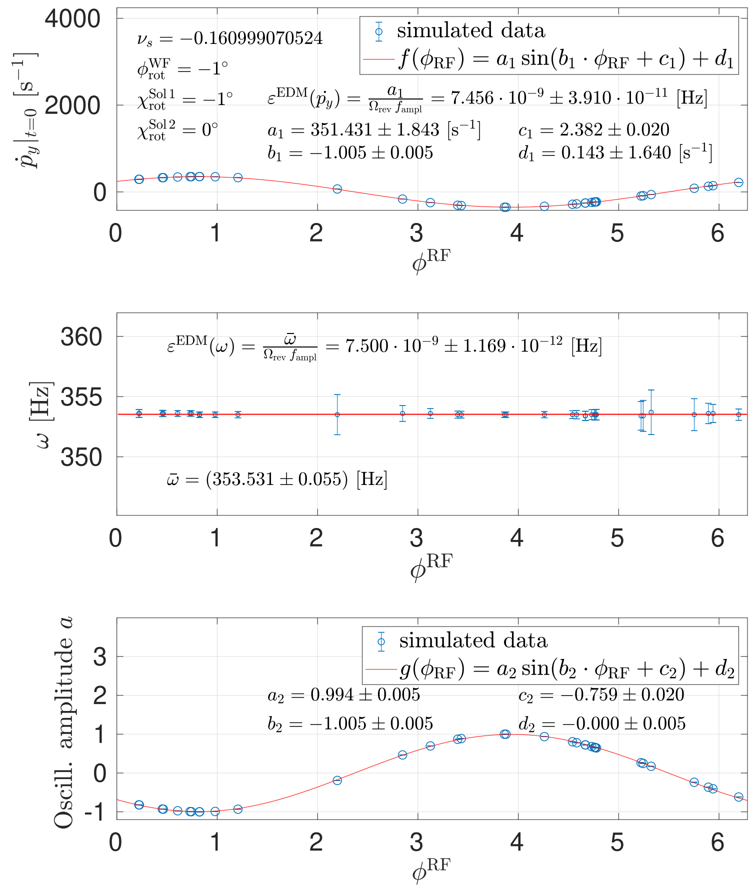

Figure 3: Simulation for one specific combination of the RF Wien filter and solenoid spin rotation angles $(\phi^{\rm WF}_{\rm rot}, \chi^{\rm Sol\,1}_{\rm rot}) = (-1°, -1°)$. 36 random values of $\phi_{\rm RF}$ are used to obtain the resonance strengths $\varepsilon^{\rm EDM}$ from the sinusoidal oscillation of $p_y(t)$ (see Fig. 18 of [5]). Depicted here as function of the randomly chosen $\phi_{\rm RF}$ are the extracted initial slopes $\dot{p}_y(t)|_{t=0}$, $\omega = \Omega^{p_y}$, and the amplitude a of the p_y oscillation (see Eq. (108) of [5]). The parameters used for the calculation are $n_{\rm turns} = 2 \times 10^4$, $n_{\rm points} = 200$, and $d = 10^{-20}$ e cm. For the beam, the conditions of Table I of [5] apply. The RF Wien filter is operated at harmonic $K = -1$.

can be somewhat reduced, which shall lead to an increased duty cycle with respect to the determination of $\varepsilon^{\rm EDM}$.

The approach to determine $\varepsilon^{\rm EDM}$ based on the oscillation frequency offers two new distinct benefits over the determination based on the initial slope alone. Firstly, it becomes possible to investigate systematic effects that appear *during* the buildup process by inspecting ω as function of time in the cycle. Secondly, having available also the amplitudes of the polarization oscillation (lower panel in Fig. 3) from a fit to $p_y(t)$, one can provide a direct comparison of $\varepsilon^{\rm EDM}$ extracted from the two methods.

2.3.2 Maps of $\varepsilon^{\rm EDM}$ using both solenoids available at COSY

The spin evolution, *e.g.*, described by Eq. (1), depends on the location of the solenoid in the machine that is used for the measurements. Therefore, making a measurement with the Siberian snake solenoid *and* the 2 MV electron cooler solenoid, shall allow us to independently determine the orientation of the invariant spin axis from the two obtained maps.

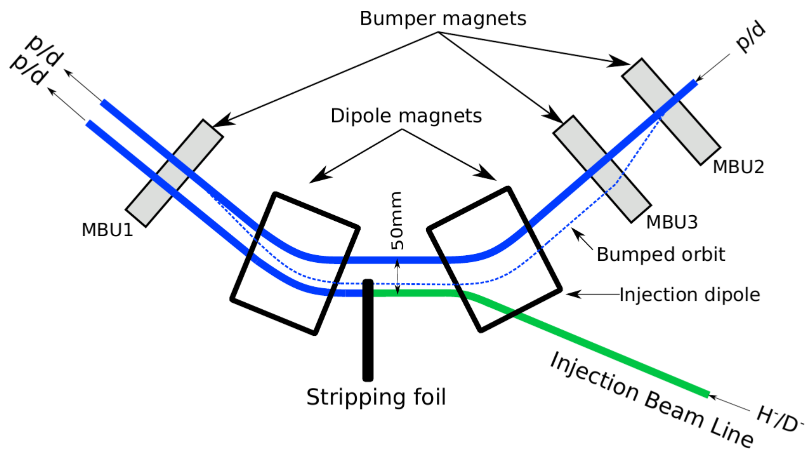

Figure 4: Sketch of injection in COSY. The beam coming from the injection beam line is shown in green, the circulating COSY beam is shown in blue. After hitting the stripping foil, the injected H^- or D^- ions loose their electrons and become protons or deuterons. (Figure taken from Ref. [Figure 2.7][11].)

3 Improvements for the 2$^{\text{nd}}$ run

3.1 Technical improvements at COSY

An ambitious program has been initiated to enhance the beam diagnostics capabilities at COSY with respect to, *e.g.*, beam position, machine tune, and chromaticity. In the subsequent sections, various of these topics are addressed.

3.1.1 Potential improvements of the injection into COSY

Progress has been made with respect to the injection into COSY, and details can be found in the recent Master's thesis [11]. In the following, some of the issues are discussed.

Negatively charged H^- or D^- ions from the pre-accelerator JULIC are transported via a 94 m long transfer line to one of the 24 dipoles (MD 23) of the race-track type COSY ring. The ions are entering the magnetic field at the open side of the C-type rectangular dipole magnet. Inside the dipole, they are bent in opposite directions toward the orbit such that at the exit, the ions are moving at a distance of about 50 mm parallel to the orbit, and are eventually stripped by the target foil, located about 0.3 m away from the dipole border (see Fig. 4). As indicated in Fig. 4, the bumper system shall ideally provide a symmetric three-bumper orbit excursion to facilitate injection of the fully stripped ions.

The COSY dipoles were designed according to the basic specification of 15° deflection at a nominal bending radius of $\rho = 7$ m. The nominal orbit of COSY was thus determined by 24, 1.8326 m long pieces of arcs with appropriate straight section between them. The effective length ℓ_z^{eff} (magnetic length along the center line) of such a rectangular dipole should therefore be 1.8274 m. All fabricated dipoles have $\ell_z^{\text{eff}} = (1825 \pm 1)$ mm, whereby the bending radius is reduced to 6.990 92 m. Given a momentum of 0.462 374 GeV/c requires at present an actual value of the magnetic field of $B = \frac{3.33564 \cdot p}{\rho} = 0.220\,62$ T. Tables of the original calibration measurements performed in 1990 provide the necessary excitation current to achieve $B = 0.220\,62\,\text{T} \Rightarrow I = 494.06$ A. At COSY at present, however, a typical starting value of 491 A is used. As a consequence of this, the orbit in the arcs are distorted, yielding to horizontal excursions of up to 40 mm from the ideal orbit. As a first

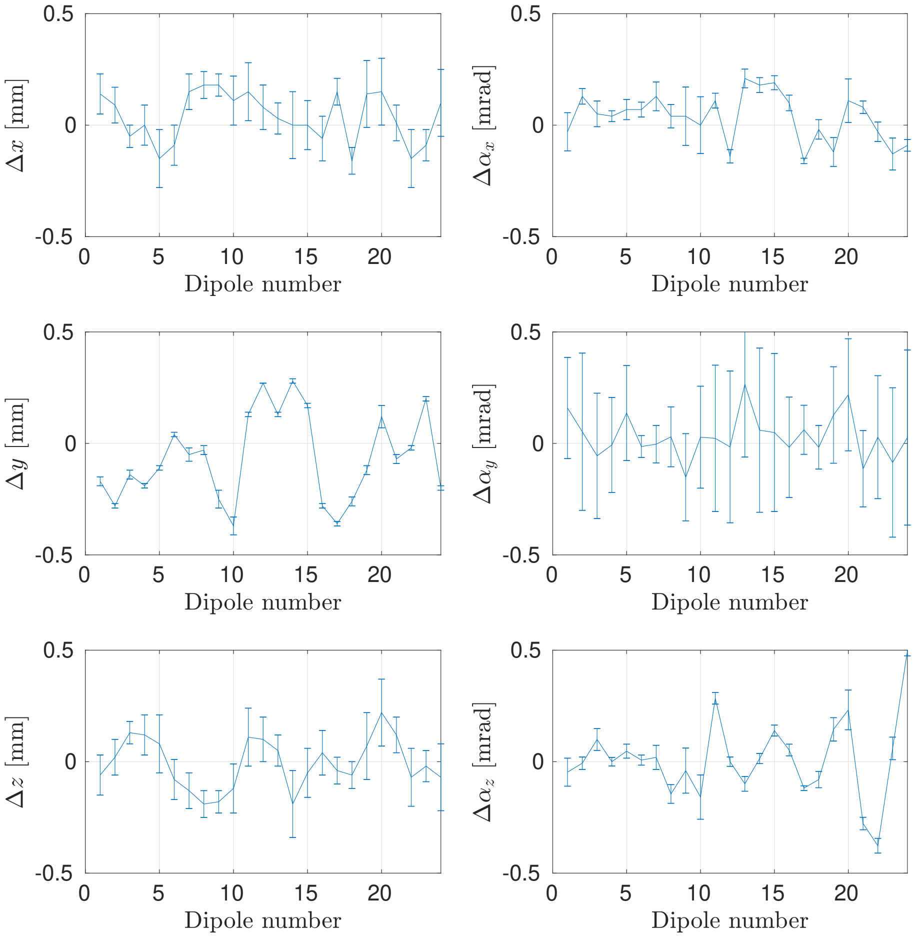

Figure 5: Translation parameters of 2019 (Δx, Δy, and Δz) and rotation parameters ($\Delta\alpha_x$, $\Delta\alpha_y$, and $\Delta\alpha_z$) for each of the 24 dipole magnets of COSY, including uncertainties derived from the measurements [12].

recommendation, the dipole start current should be increased to the value given above. Then also the position of the stripping target should be changed from the present -58 mm to -45 mm, *i.e.*, closer to the nominal orbit.

3.1.2 Alignment campaigns of the COSY magnet system

There have been various surveys and alignment campaigns conducted at COSY during the past years. An example of the results of the dipole parameters are shown in Fig. 5. It should be emphasized that the uncertainties of these parameters are of the order of ≈ 0.3 mm and ≈ 0.3 mrad. Similar results have been obtained for the translational and rotational parameters of the quadrupole magnets in COSY.

3.1.3 Beam-based alignment

The beam-based alignment effort, primarily motivated in order to improve the JEDI precursor experiment on the deuteron EDM at COSY, has been performed in two beam times, where in the first beam time in February 2019 (Experiment A15), a smaller subset of the quadrupoles has been measured [13], and in September/October 2019 (Experiment A15.1) all the quadrupoles have been measured [14]. For the September/October 2019 measurement the hardware in COSY needed to be upgraded, as the quadrupole magnets

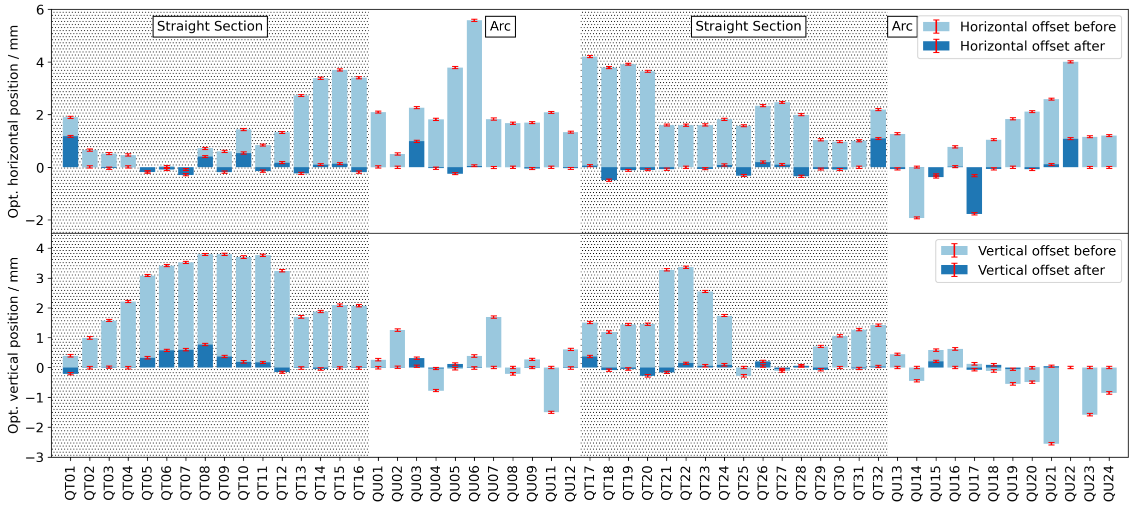

Figure 6: The optimal beam position in all quadrupoles. The top part shows the horizontal direction and the bottom part the vertical one. The optimal position inside the quadrupoles before the BPM calibration is depicted with light blue color, and after the BPM calibration it is shown in dark blue color. The error of the optimal positions is 40 µm, as indicated by the red error-bars. For a more detailed explanation, please see Ref. [14].

are powered in series, which does not allow an individual modification of the strength of one quadrupole. This has been achieved by additional power supplies[2] that can be connected in parallel and be used to add or bypass some current for a single quadrupole.

As a result of the beam-based alignment, a beam-position monitor calibration could be obtained, which moves the quadrupole centers onto or close to the zero line of the coordinate system (see Fig. 6). This makes the corrected orbit pass close to the centers of the quadrupoles. The overall improvement of the closed-orbit could be confirmed by the fact that after the beam-based alignment procedure was applied, less steerer correction power is needed to reach the optimal orbit, as one does not have to act against the steering effects from off-center quadrupoles. For the vertical direction, this amounts to about 80% less and for the horizontal direction to about 20% less required steering power.

Apart from a better orbit in the machine, also misalignments of quadrupoles were observed and confirmed with additional mechanical measurements. Those observed quadrupole misalignments will be corrected in the future, and lead to further improvement of the accelerator performance.

3.1.4 Improvements of COSY signals and distribution

10 MHz **synchronization of relevant RF devices:** A GPS-driven 10 MHz signal is now used to synchronize all frequency-related devices in COSY including the experiment installations.

Especially important is the synchronization of the frequency generators for the COSY cavity, the RF solenoid and the RF Wien filter. Both, the RF solenoid and the RF Wien filter have to operate at a harmonic of the COSY revolution frequency $f = f_{\mathrm{COSY}}|\nu_s + n|$, where ν_s is the spin tune and n an integer number. With individual oscillators for each device, the resonance condition had to be retuned at least once per day by an amount of

[2]Model NL20V20C40, bipolar - 4 quadrant power supply, Höcherl & Hackl, https://www.hoecherl-hackl.de/

the order up to some 10 mHz (10^{-7} to 10^{-8} relative), which is 1 to 2 orders of magnitude larger than the typical cycle-by-cycle variation of the spin tune (see Fig. 4 of Ref. [15]).

A change in frequency results in running slightly off-resonance. In case of the RF solenoid, which is used to rotate the spins after injection into the horizontal plane, this means incomplete or too large rotations and, thus, different starting conditions for the EDM measurement. This circumstance adds further systematic uncertainties. With the new frequency synchronization enabled, no retuning was necessary during the last long-running experiment (Axion search, COSY Experiment E008, see Ref. [16]).

Reference Frequency Distribution: The Fiber-Optics-based Reference Frequency Distribution System (**FO-RFDS**), recently implemented at COSY, is a system that distributes up to four reference frequencies through fiber optic cables from signal source devices (frequency generator, arbitrary waveform generators) to relevant systems of the EDM experiment, where a clean frequency signal with a low-phase noise and a high signal-to-noise ratio is required.

Through fiber-optic cables, signals and data can be transported over short and long distances, as well as with a low and high bandwidth, depending on the application. Fiber optic cables are electromagnetically not radiating and they are immune to interference and grounding issues.

With such an optical signal transport and distribution, source generators of TTL[3] and/or Sine-wave signals are electrically decoupled from their destination systems. Electrical decoupling prevents noise contamination to the signal and noise propagation through cross-talks, interference, pickups, and ground-loops. Electrical decoupling is insured by optocoupler devices like transmitters and receivers. This approach ensures the cleanliness of the signals during their transport and during arrival at the target destinations. With transceivers, the electrical signal is converted to an optical signal and subsequently transported through optical fibers. Close to the target system, the optical signal is converted back to electrical signal (mainly TTL) to be fed to the destination devices. The basic principle of the FO-RFDS is illustrated in Fig. 7.

The four reference frequencies, labeled RF_A, RF_B, RF_C, RF_D, and their source generators are listed below. For an illustration of the scheme, implemented at COSY, see Fig. 8.

- $\mathrm{RF}_A = 10\,\mathrm{MHz}$: Synchronization frequency: TTL signal generated by a very precise GPS timing receiver[4].

- $\mathrm{RF}_B \simeq 750\,\mathrm{kHz}$: COSY-frequency. Sine waveform generated by the COSY master clock (IKP internal R&D).

- $\mathrm{RF}_C \simeq 871\,\mathrm{kHz}$: Solenoid frequency: Sine waveform generated by a Rohde & Schwarz SML 02[5].

- $\mathrm{RF}_D \simeq 871\,\mathrm{kHz}$: Wien-Filter frequency: Sine waveform generated by an arbitrary 8-channel waveform generator from Zurich Instrument[6].

[3]TTL: transistor-transistor logic

[4]LL-3760 GPS Timing Receiver, Lange-Electronic GmbH, 82216 Gernlinden, Germany, https://www.lange-electronic.de/en/products/high-end-time-and-frequency/ll-3760-gps-timing-receiver-detail.

[5]Rohde & Schwarz, 81671 München, Germany, https://www.rohde-schwarz.com/se/product/sml-productstartpage_63493-7567.html.

[6]HDAWG 750 MHz Arbitrary Waveform Generator, Zurich Instruments AG, 8005 Zurich, Switzerland, https://www.zhinst.com/others/products/hdawg-arbitrary-waveform-generator

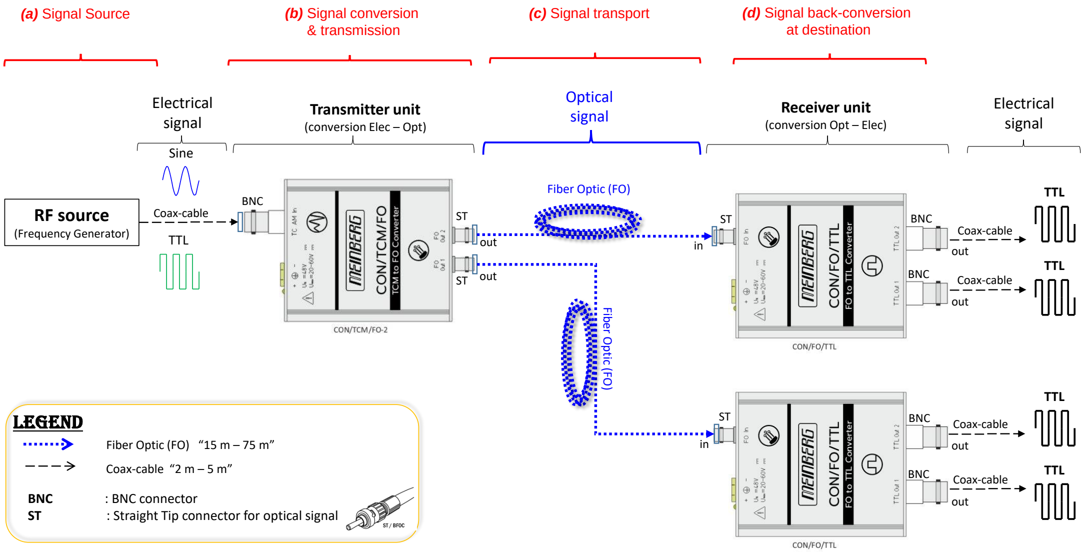

Figure 7: Synoptic scheme of the principle of Electrical signal (TTL/Sine) conversion to optical signal (transmitter unit), optical signal transport over optical fibers, conversion back from optical signal to electrical signal (TTL)

3.1.5 New tool for fast tune and chromaticity measurements

Measurements of the betatron tune are crucial for the operation of circular particle accelerators. The tune must be monitored in order to avoid resonances causing beam instabilities during acceleration that limit the lifetime of the stored particle beam. A fast tune measurement system based on bunch-by-bunch beam position measurements was recently developed at COSY. Betatron oscillations of the beam are excited through stripline electrodes with an appropriate RF signal. Resonant transverse oscillations are then observed using the capacitive beam position pick-ups at COSY and the Libera-hadron readout modules of the beam-position monitors (BPMs). This system allows not only for a fast tune measurement within a few milliseconds, but also enables *continuous* tune monitoring during beam acceleration and operation. The high precision tune measurement also makes possible the determination of the beam chromaticity. Therefore, the particle momentum is changed by means of a small frequency change. The consequential tune change is observed and provides a precise measure for the chromaticity.

The fast tune measurement system is already being used in daily operation at COSY. The chromaticity measurement system was recently commissioned successfully and is now available for routine use (see Fig. 9).

It should be noted that although the JEDI experiments have led to a good understanding of how spin-coherence time can be optimized at COSY (see, *e.g.*, Ref. [17]), the experimental data base that connects beam chromaticity, beam emittance and spin-coherence time is scarce. In particular for the future investigations eventually aiming at a measurement of the proton EDM, the new fast tune and chromaticity tool developed at COSY will become indispensable.

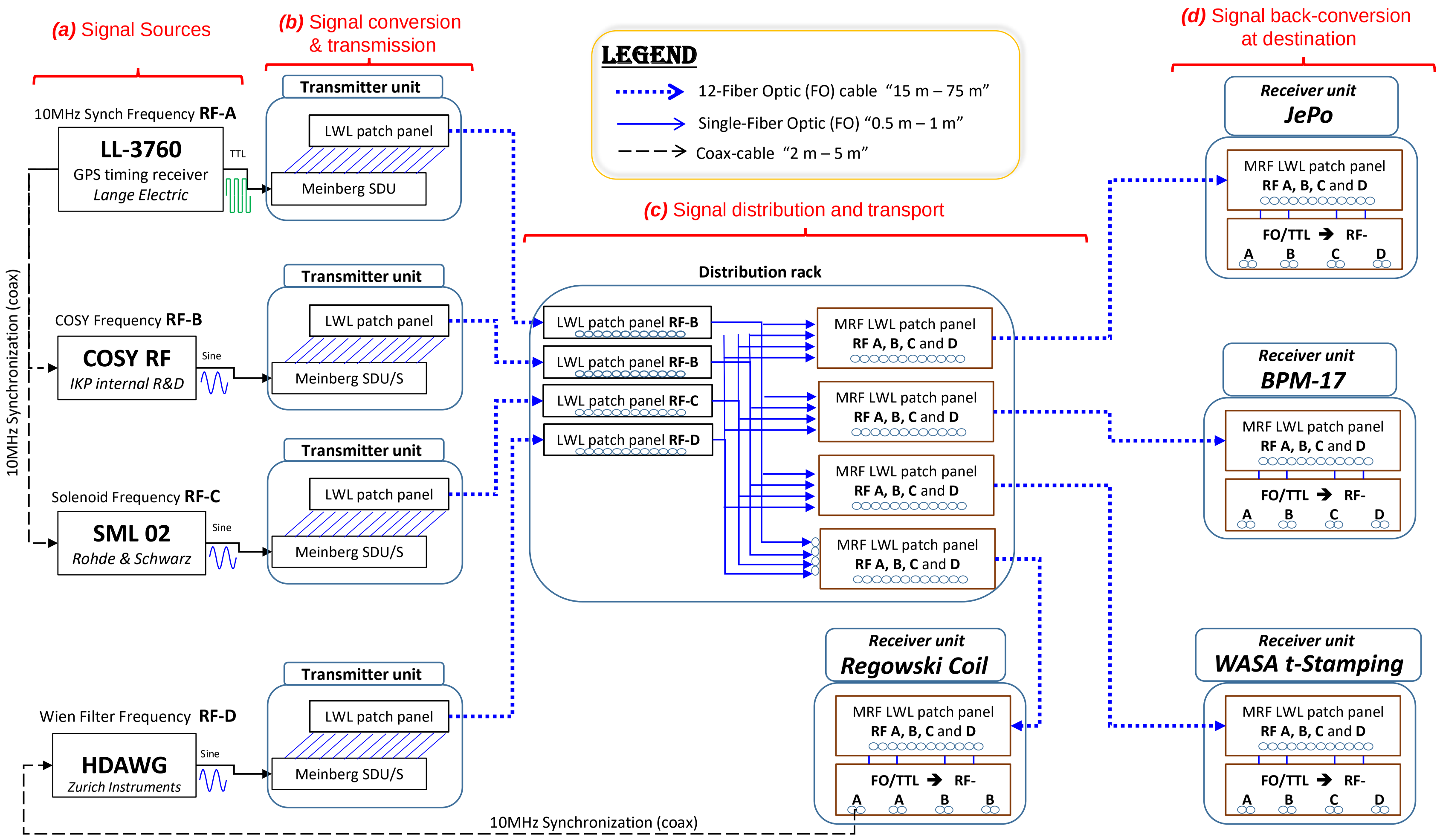

Figure 8: Scheme for the distribution of reference frequencies based on fiber optics **FO-RFDS**, implemented for the JEDI experiment at COSY.

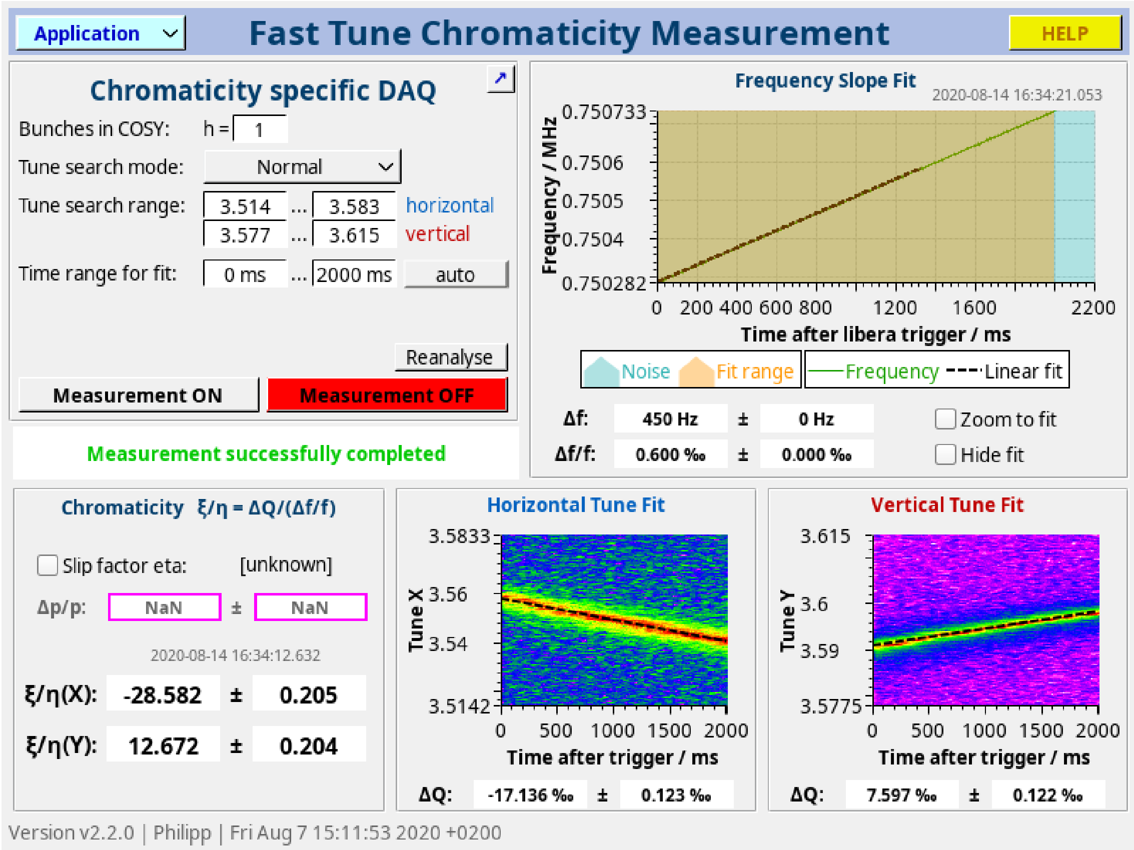

Figure 9: Screenshot of the control panel for fast tune and chromaticity measurement at COSY.

3.2 New JEDI Polarimeter

The development of a new beam polarimeter is motivated by the need to provide a polarimeter system for storage ring EDM experiments that is compact and in principle capable to determine efficiently polarizations for clockwise and counter clock-wise beams. In addition, compared to existing polarimeters, the detection scheme based on energy loss using LYSO crystals appears simple (for details, see Chap. 11.8, "Development of calorimeter detectors for an EDM polarimeter" of Ref. [7]). Another aspect of this development, not discussed here in detail, is the need to provide for storage ring EDM searches a possibility to determine the polarization profile of the beam. First ideas about how this could be accomplished are summarized in Appendix K of Ref. [7].

As it is currently installed in COSY, the new JEDI polarimeter (JEPO) consists of 52 LYSO-SiPM modules in the cross configuration. The polarimeter is capable to cover scattering angles from 4° to almost 13° degrees in the laboratory. The detector has two layers: 2 cm thick plastic scintillator ΔE detector followed by 8 cm thick LYSO crystals [18]. The readout of the whole detector is done by SiPM sensors. The power supply of the sensors is custom made using high-precision voltage regulator boards. The polarimeter is equipped with two 2 cm thick carbon block targets that can be inserted into the beam along the vertical and horizontal direction. The targets can approach the beam from the upper and left sides (look in beam direction), and then the resonant plus white noise extraction moves the beam particles close to the target. All systems are remote controlled and can be operated in automatic mode. A fast 250 MSPS digitizer does the readout of all crystals with a 14-bit resolution. The same system has time-stamping capability,

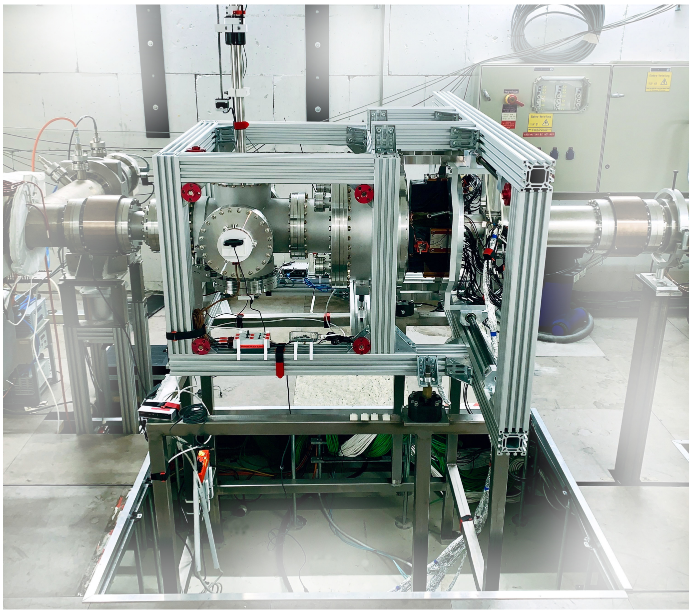

Figure 10: The new JEDI polarimeter (JEPO) installed in the target section (former EDDA location) downstream of the RF Wien filter at COSY. The beam direction is from left to right. From the left, the first flange is a target chamber with a 2 cm thick carbon target. Subsequently, the vacuum flight chamber is seen and at the right LYSO-SiPM modules.

which can be used to monitor the spin precession of the particle (see, *e.g.*, Ref. [15]). The downscaled signals from the COSY RF cavity, RF solenoid, and RF Wien filter are fed into the readout system.

All this makes JEPO a very versatile detector system that can be used continuously during long beam times. Up to now, the polarimeter has been successfully used during commissioning beam times, as well as for regular JEDI experiments.

3.3 Improvements at the RF Wien filter

The original design of the waveguide RF Wien filter for the EDM measurements of protons and deuterons at COSY is described in Ref. [9]. The driving circuit of the Wien filter is discussed in Ref. [19]. A general application of the polynomial chaos expansion (PCE) method as a tool to evaluate and quantify field homogeneities in the RF Wien filter is discussed in Ref. [20]. The PCE method is well-suited to provide a quantification of errors in high-precision experiments.

Below, a number of recent technical improvements of the RF Wien filter are discussed.

3.3.1 8-channel Zurich Instruments signal generator

During the design phase of the RF Wien filter, we decided to use four power amplifiers (PA) to feed the four input electrodes of the Wien filter instead of combining them and re-splitting of the power. These PAs are driven by a single signal generator (SG), where its output is splitted into four signals by a passive (*lossless*) power divider. The use of four separate PAs means that the driving circuit has to cope with a multitude of different amplitude and phase responses of each PA. As a consequence, a sightly inhomogeneous feeding signal will propagate along the electrodes, which when combined excite a slightly inhomogeneous electric and magnetic field. Additionally, when these signals combine, some

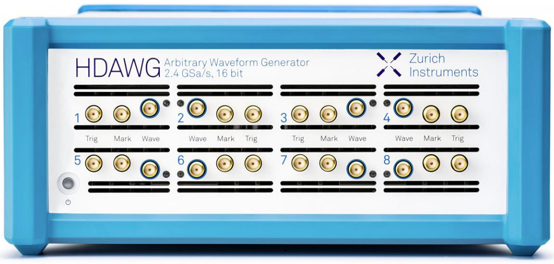

Figure 11: A photograph of the 8-channels High-Definition Arbitrary Wave Generator (HDAWG) from Zurich Instruments[6].

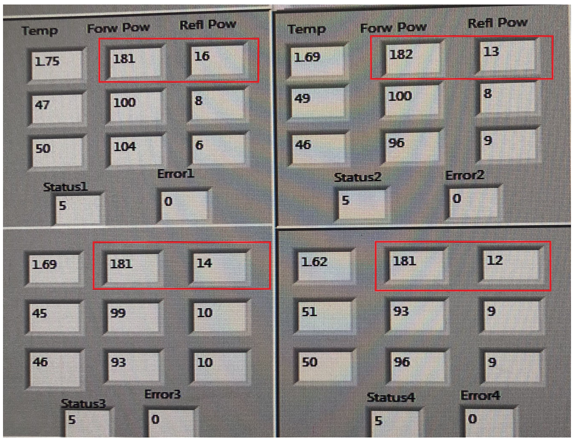

Figure 12: A photograph of the slow-control monitoring user interface of the power amplifiers, showing the forward and reflected power of the four input ports to the RF Wien filter highlighted in red.

power loss up to 10% has been observed. Some of these power RF signals are reflected back to the amplifiers, which reduces their operation time before they shut-down for safety reasons.

Alternatively, we tried to use multiple SGs, each driving a single PA. This provides the possibility to control the amplitude and phase of each PA independently. We tried this option, but unfortunately, we could not synchronize the SGs.

The solution we finally succeeded to implement was to use a SG that provides multiple internal channels such as the HDAWG from Zurich Instruments[6], shown in Fig. 11. What is so special about this device, is that multiple-output channels can be linked to a single numerical oscillators. This implies an inherent synchronization process, which has meanwhile been tested successfully.

Offline test of the ZI SG were successfully performed. In order to generate an RF power of $\approx 660\,\mathrm{W}$ at $871\,\mathrm{kHz}$, for instance, setting the amplitude and phase at the SG to:

- Channel-1: $0.263\,\mathrm{V},\ 0\,\mathrm{deg}\,,$
- Channel-2: $0.253\,\mathrm{V},\ -3\,\mathrm{deg}\,,$
- Channel-3: $0.242\,\mathrm{V},\ 180\,\mathrm{deg}\,,$
- Channel-4: $0.255\,\mathrm{V},\ 178\,\mathrm{deg}\,.$

The above scheme provides a uniform feeding signal, as can be seen in Fig. 12. Tests with beam are going to be carried out during the September 2020 JEDI run at COSY.

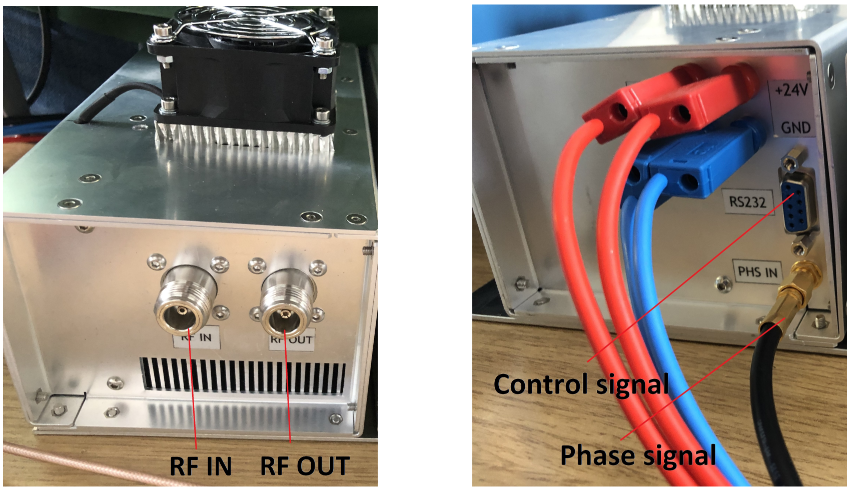

(a) Front view. (b) Rear view.

Figure 13: Photographies of the fast RF switches show in the high-power interfaces, 'RF IN' and 'RF OUT' and the phase signal used to delay the output in addition the control signal.

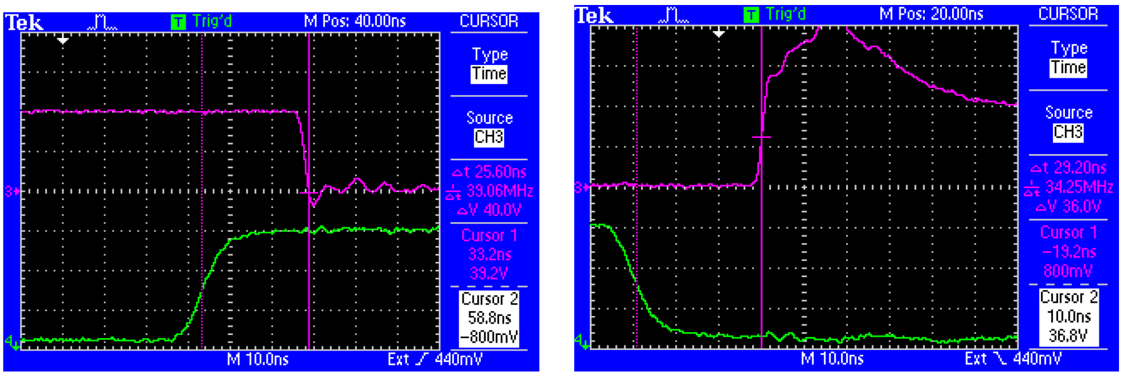

(a) Switching RF on. (b) Switching RF off

Figure 14: Offline test of the fast RF switches.

3.3.2 Fast RF switches

In order to enable the RF Wien filter to manipulate the spin of individual bunches stored in the machine, the driving circuit was equipped with custom-designed RF switches, shown in Fig. 13.

These switches are in principle able to handle up to 500 W each, which permits the system to run near a total power of 2 kW in pulsed mode.

Figure 14 shows offline test results of the switches when they are switched off (panel a) and on (b), respectively. The including the internal delay between the driving circuit and the RF transistors, approximately, the switches need 25 ns to go into the 'low state'. The actual switching-off time is less than 10 ns. On the other hand, the switches exhibit some delay of approximately of 19 ns. In conclusion, the aforementioned numbers should be sufficient to run the RF Wien filter in a way to have a pilot bunch, which will enable us to conduct a frequency-based EDM measurement at COSY.

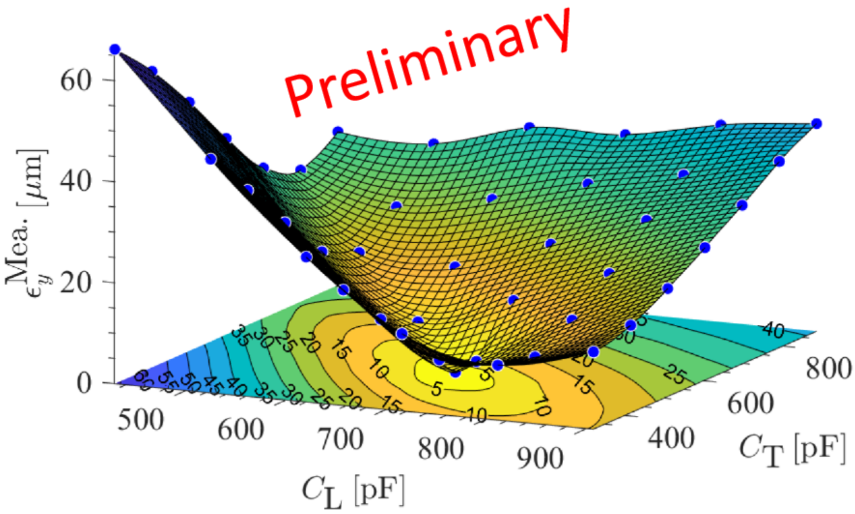

Figure 15: Preliminary data of the measured amplitudes of beam oscillations ϵ_y as a function of the variable capacitor values C_{L} and C_{T}.

3.3.3 Improved matching of the RF Wien filter

The Wien filter, in principle, should be able to generate RF electric and magnetic fields so that the corresponding Lorentz force exerted on the beam vanishes. The Lorentz force, in this context, is quantified in terms of the amplitude of the induced beam oscillations, when the forces are mismatched. Figure 15 shows the measured values of the amplitude of these induced beam oscillations as a function of two variable capacitors, C_{L} and C_{T}. Each combination of these capacitors corresponds to a well-defined case of electric and magnetic forces. We were able to match the RF Wien filter so that the minimum measured amplitude of beam oscillations read 1 μm at a conventional COSY BPM, nearly 70 m away from the RF Wien filter. This value is amplified by the square root of the ratio of the beta-functions at these two locations. This value corresponds to the smallest point that we could measure with the available BPM readout electronics based on lock-in amplifiers[7]. The spin dynamics simulations, however, have shown indeed that an oscillation amplitude that is at least one order of magnitude smaller could be obtained, still within the capabilities of the driving circuit. The effect on the EDM measurements is yet to be investigated in more detail in the future.

The data on RF Wien filter induced oscillations, shown in Fig. 15, are presently evaluated in much more detail, with the goal to understand how close we are already to the quantum limit.

3.3.4 Optimization of Rogowski BPM system

A new type of Beam-Position Monitor (BPM), based on a Rogowski coil design [21], has been recently developed at the IKP of FZ-Jülich. These pick-ups are presently in a development stage. One of the primary advantages of these BPMs is that they require only a very short beam insertion length of $\approx$ 60 mm and provide an offset-bias free response to

[7] HF2LI 50 MHz Lock-in Amplifier, Zurich Instruments AG, 8005 Zurich, Switzerland, https://www.zhinst.com/others/products/hf2li-lock-amplifier.

counter-circulating beams, which makes these instruments attractive as BPM candidates for EDM storage rings.

The Rogowski BPMs used at the entrance and exit of the RF Wien filter so far in COSY had turn number and self resonance frequency[8] (for single quadrant coil) of 445 and 1.2 MHz, respectively. With these specifications, the BPMs were well-suited for the operation in single bunch mode at the typical JEDI deuteron beam momentum of 0.97 GeV/c, corresponding to a beam revolution frequency of 750 kHz. For COSY beam in four-bunch mode, a new Rogowski BPM has to be developed, where the operational bandwidth is at least a factor of three higher. One possibility to increase the frequency bandwidth (keeping the geometrical parameters of the torus unchanged) is to use a thicker wire for the windings of the coil which in turn results in decreased number of windings. This can help to decrease overall inductance of the coil by a factor corresponding to the fractional change introduced in the turn number and hence, to increase the natural frequency of the system by the same factor[9].

The wire diameter of the windings was increased from 140 to 400 µm. Thereby, the angular winding coverage was decreased from about 90° to around 60°, which resulted in overall single-quadrant turn number of 132 [see Fig. 16(a)]. Mechanical or human-related imperfections mainly induced during winding of the four quadrants or during the assembly process, where electrical connections are made with the help of twisted-pair wire extensions, can introduce unwanted (non-ideal) effects on the resonance curves of the four quadrants, leading to a situation, where the individual quadrant coils do not resonate at the same frequency[10]. In order to improve this, an adjustable capacitor [see Fig. 16(b)] was connected in parallel with each quadrant coil (just before amplification). In an attempt to get the system of four quadrants resonating at the same frequency, the trimmers were adjusted by introducing capacities of a few pF[11]. Figure 17 shows the frequency dependence of the four quadrants of the Rogowski BPM before [17(a)] and after [17(b)] tuning the system to resonate at 3.229 MHz. The tuning was successfully accomplished with a phase shift of less than 1° on resonance for all quadrants. Obviously, the distortions in both amplitude and phase response were greatly minimized by the tunable capacitor system.

After tuning the four-quadrant system, the Rogowski BPM was calibrated by scanning a two dimensional map in a range of (± 10 mm $\times$ ± 10 mm) with a step size in each direction of 1 mm. A comparison between the measured positions and those reconstructed from theoretical expectations for two calibration measurements (performed at 750 kHz and 3 MHz) is illustrated in Fig. 18. Based on 441 data points, the distributions of the differences for horizontal and vertical beam coordinates exhibit a resolution of < 100 nm for the lower frequency case and of several hundred nanometer for the calibration at 3 MHz. The discrepancy between the two cases can be attributed to the higher electromagnetic interference between individual quadrants as the frequency gets larger.

[8] Measured for the complete realistic single-quadrant system, including effects from cabling, as well as pre-amplifiers.

[9] The inductance is proportional to the square of the turn number, while the self resonance is inversely proportional to the square root of the inductance [22, 23, 24].

[10] The system lumped elements are sensitive to, for example, an uneven spacing between individual quadrant windings or an possible unequal length of the twisted-pair wire extensions.

[11] Each quadrant required a unique capacitance as all quadrants were showing slightly different frequency curves with their original circuits.

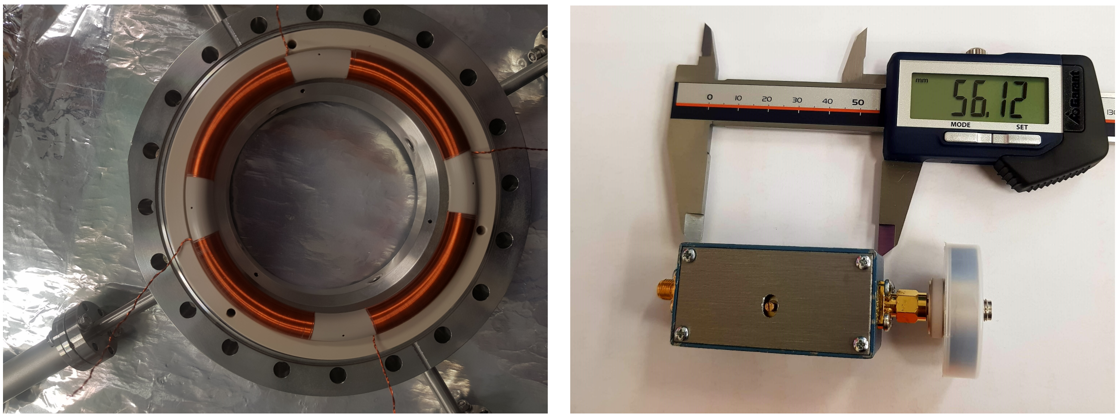

(a) Winding of Rogowski BPM with higher bandwidth.

(b) Adjustable capacitor (trimmer) for tuning quadrants.

Figure 16: (a) Winding of the Rogowski BPM with higher bandwidth. Each quadrant coil has 132 turns and covers an angular range of around 60°. (b) Adjustable capacitor (trimmer) used in parallel connection with each quadrant coil in order to tune the four-quadrant system at 3.229 MHz.

3.3.5 Upgrade of slow-control system

In order to implement the 8-channel Zurich Instruments signal generator[6] and the fast RF switches in the input ports to the RF Wien filter, the slow control system has been upgraded.

8-channel Zurich Instruments signal generator: The 8-channel Zurich Instruments signal generator is controlled by slow control via Ethernet: The parameters that are controlled are the frequencies, the signal amplitudes, the phase shifts, the status bits (on/off), and the enable switches that activate the output of each of the 8-channels. All the channels are forced to have the same frequency, the frequency can be either adjusted manually or tuned automatically with a signal from the beam polarization measurement, that determines the spin-tune, and hence the in-plane spin precession frequency in the machine. The software controls also the phase shifts in order to keep the first two channels at $\approx 0°$ phase shift, while channels 3 and 4 shall have a $\approx 180°$ phase shift, the channels from 4 to 8 shall have also a 0° phase shift. The RF amplitude (in Volt) will be adjustable manually in steps of 100 µV. A screenshot of the slow-control interface screen is shown in Fig. 19(a).

Fast RF switches: The four RF switches are controlled by the National Instrument Compact RIO (cRIO) system via the module NI9870 that is already in used to control the other basic function of the RF Wien filter. The NI9870 is a serial interface module which adds 4 serial ports to the cRio system, the serial ports have a coordinate access to the cRIO FPGA. All the four switches are controlled in parallel in order to offer the maximum speed, when the parameters are changed. The slow control will allow to enable and disable to output, to set the levels of the output high or low, to change the phase shift, and to control the internal temperatures, and the status of the RF switches. A screenshot of the slow-control interface screen is shown in Fig. 19(b).

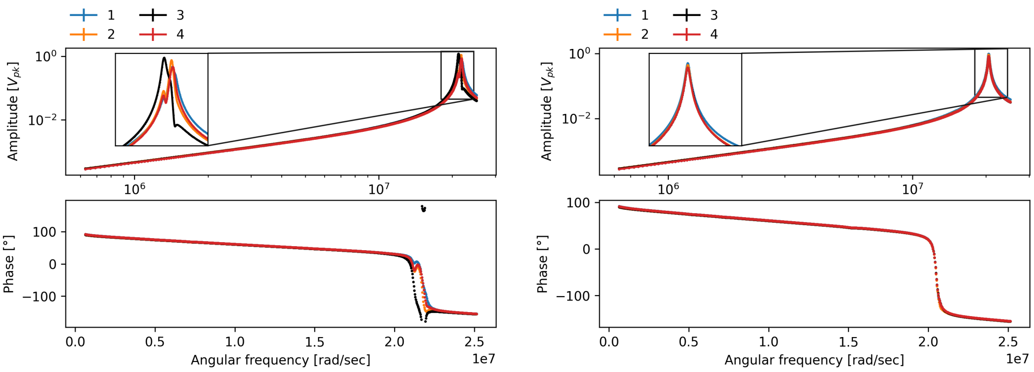

(a) Measured frequency response before tuning. (b) Measured frequency response after tuning.

Figure 17: Measured frequency response of the four quadrants before (panel a) and after (b) tuning. The inserts in the upper plots show voltage amplitudes in a logarithmic scale. The lower subplots show phase responses in a linear scale. The numbers in the legends indicate the quadrant number.

3.4 Other aspects

3.4.1 Determination of unwanted magnetic fields in COSY

Effect of the bump on the spin tune: The spin tune denotes the number of spin rotations in one turn of a particle in the ring. It can be determined to a very high precision, with a relative error of 10^{-10} during a 100 s long beam cycle [15]. Such precision allowed us to develop a new method, called "spin tune mapping"[25]. It is based on the measurement of the spin tune shift with respect to different artificial imperfection fields created in the ring. The spin tune shifts can be predicted by a model and then the model parameters can be determined. Experimentally, in the new approach, proposed here, we suggest to use steerer fields (assuming the role of those artificial imperfection fields) in a predictable manner, namely creating local vertical closed orbit bumps[26]. At COSY there are 11 options right now to create such vertical bumps.

The bumps are produced by three consecutive vertical steerers. In order to keep the bump a closed one at all magnitudes of the bump, the steerer kicks must be kept proportional to each other. The proportionality coefficients would depend on the betatron phase advances and beta functions in the steerers. The spin rotation in the bump is predicted by spin tracking using COSY-Infinity [27]. It is similar to that caused by a weak helical snake. Effectively, it produces a spin kick around a fixed in-plane axis $\vec{w} = \vec{e}_x \sin\alpha + \vec{e}_z \cos\alpha$, where α is a directional angle that is counted from the positive axis z towards the positive axis x. The magnitude of the spin kick ψ in the bump is proportional to the steerer kick angle θ of a central steerer in the bump which is chosen as a reference one. The bump amplitude is also proportional to θ. Both analytic and lattice models predict that the spin tune has a parabolic dependence on the bump amplitude (see Fig. 20). The corresponding analytic result for the relative change of the spin tune $\Delta\nu_s$ of stored beam at the moment when the bump steerers are switched on, is

$$\cos\pi(\nu_s + \Delta\nu_s) = \cos\pi\nu_s \cos\frac{\psi}{2} - (\vec{c}\cdot\vec{w})\sin\pi\nu_s \sin\frac{\psi}{2} \tag{5}$$

where $(\vec{c}\cdot\vec{w}) = c_x \sin\alpha - c_z \cos\alpha$ defines the offset of the minimum of a parabola. The components of the invariant spin axis c_x and c_z are defined after the last steerer of the bump. The parameter α is specific for each bump, the COSY-Infinity simulations suggest

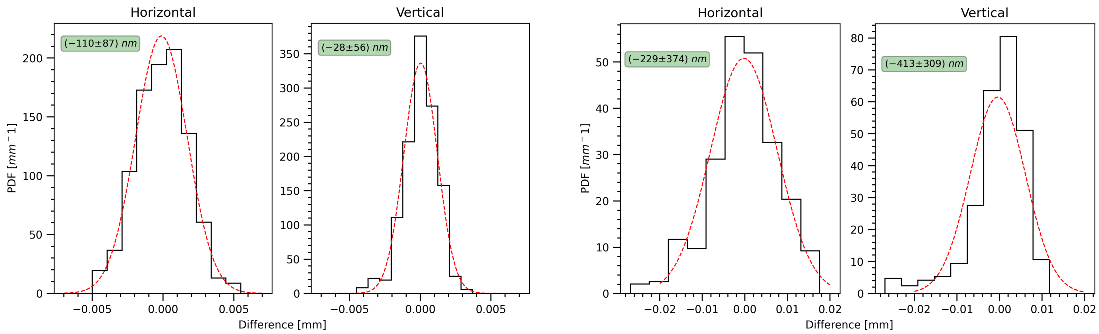

(a) Distribution of the difference between measured and reconstructed positions at 750 kHz.

(b) Distribution of the difference between measured and reconstructed positions at 3 MHz.

Figure 18: Distribution of the difference between measured and reconstructed (using theoretical model) positions at 750 kHz (panel a) and at 3 MHz (b). Gaussian fits for calibration at 750 kHz show a resolution of 87 nm and 56 nm for horizontal and vertical beam coordinates, respectively. While for the calibration at 3 MHz show a resolution of 374 nm and 309 nm for horizontal and vertical beam coordinates, respectively. Each distribution in the figure has a total 441 entries.

clustering around $\sim -40°$ or $\sim -65°$. Here we mention that the method is not sensitive to the in-plane projection of the invariant spin axis $\vec{c}$ should it be orthogonal to $\vec{w}$ of a particular bump.

In the measured spin tune shifts produced by the bump, there are only two parameters used in the analytic model: the parabolic curvature and the location of the minimum controlled by the cosine of the opening angle between $\vec{c}$ and $\vec{w}$,

$$(\vec{c} \cdot \vec{w}) = \cos\angle(\vec{c}, \vec{w}) \ = -\sin\zeta. \tag{6}$$

The angle ζ specifies by how much $\angle(\vec{c}, \vec{w})$ deviates from $\pi/2$. In the ideal magnetic ring without sextupoles, $\zeta = 0$ for any vertical bump, which means the parabola in Fig. 20 is centered at zero for any bump. The typical error of ζ, assuming the same parameters as in [25], is of the order of $\sigma_\zeta \approx 10^{-6}$ rad. The estimated sensitivity to deuteron EDM is then at least $d = 10^{-19}$ e·cm and higher. The fit of the measured spin tune shifts can be also performed directly in COSY-Infinity [27]. In this case, the lattice parameters, namely the element alignments[5], are optimized with χ^2-minimization. Such fits should be rather performed on the measured spin tune maps from all of the bumps simultaneously.

It is important that the bumps are as closed as possible, i.e., are causing the least possible perturbation of the orbit except in the bump itself. If the relative orbit shift in the ring when the bump steerers are switched on is larger than 0.2 mm, it will have an impact on the location of the minimum and will increase the systematic error at its location. Orbit shifts higher than 0.4 mm will significantly reduce the spin coherence time (SCT), because the orbit in the sextupoles is not optimal anymore for a correction of the chromaticity [17].

3.4.2 Improvements of the theoretical understanding of the precursor experiment

Precision experiments, such as the search for a deuteron electric dipole moments using a storage rings like COSY, demand for an understanding of the spin dynamics with unprecedented accuracy. In such an enterprise, numerical predictions play a crucial role for the

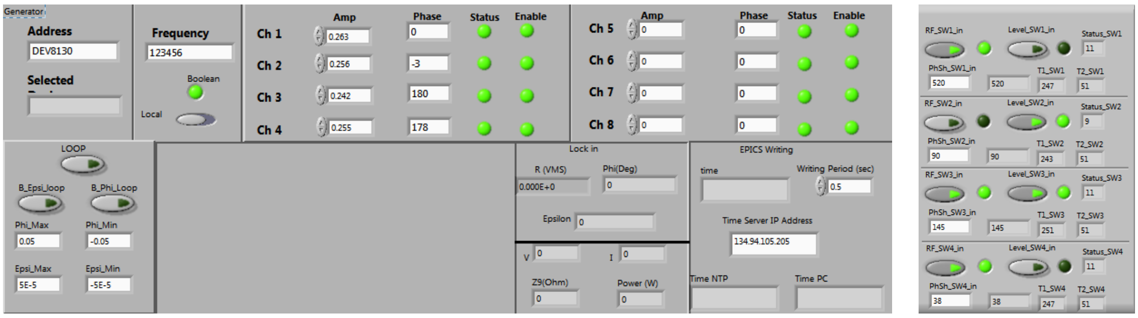

(a) Screenshot of the slow-control interface of the 8-channel Zurich Instruments signal generator.

(b) Screenshot of the GUI that controls the fast RF switches.

Figure 19: Slow control interfaces for the 8-channel signal generator (a) and the fast RF switches (b).

development and later application of spin-tracking algorithms. In a recent publication [5], various measurement concepts involving polarization effects induced by an RF Wien filter and static solenoids in COSY are discussed. The applied matrix formalism, deals *solely* with spin rotations *on the closed orbit* of the machine, and is intended to provide *numerical* guidance for the development of beam and spin-tracking codes for rings that employ more realistic descriptions of the electric and magnetic bending and focusing elements, solenoids etc., and a realistically-modeled RF Wien filter.

3.4.3 Report on "Storage Ring to Search for Electric Dipole Moments of Charged Particles – Feasibility Study"

The CPEDM collaboration has provided an extended report about the status, perspectives and strategy that shall eventually lead to a dedicated EDM storage ring of ultimate precision (see Ref. [7]). The project strategy is outlined. It foresees a step-wise plan, starting with ongoing COSY activities that demonstrate technical feasibility. Achievements to date include reduced polarization measurement errors, long horizontal-plane polarization lifetimes, and control of the polarization direction through feedback from the scattering measurements. The project continues with

(i) a proof-of-capability measurement (precursor experiment), as discussed in the present proposal, including a first direct deuteron EDM measurement,

(ii) an intermediate prototype ring (PTR) (proof-of-principle; demonstrator for key technologies), and eventually

(iii) the high-precision electric-field storage ring.

4 Beam request

The presently available data from the 1$^{\text{st}}$ run, shown in Fig. 1, were taken during a relatively short period of about six days, during which the beam conditions for the experiment were favorable. We had planned to record more data points with a smaller spacing. In addition, repetitions of each data point of the map $\varepsilon^{\text{EDM}}(\xi^{\text{Sol}}, \phi^{\text{WF}})$ were foreseen, but due to the limited running time available, these data could not be recorded. Therefore,

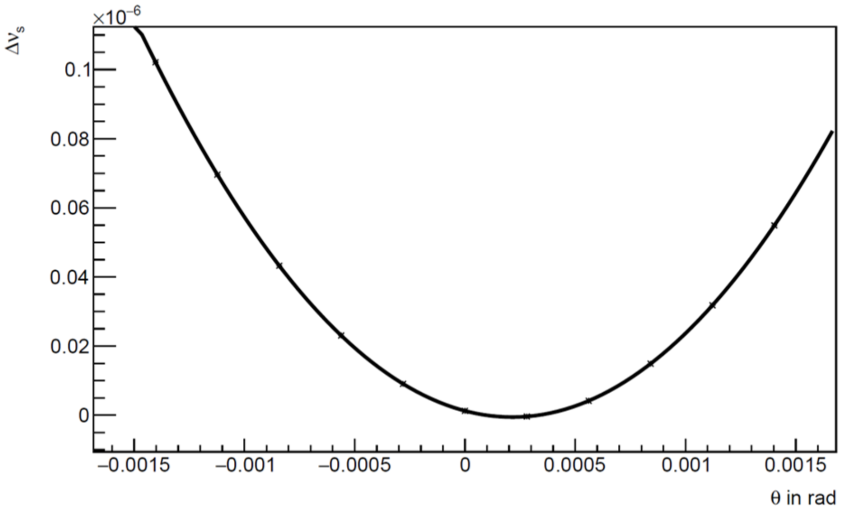

Figure 20: A model prediction of the spin tune shifts for the bump MSV 8 - 10 - 12 with respect to the kick angle θ of the central steerer (COSY-Infinity simulation with COSY lattice). The minimum is shifted because of the imperfection solenoid field of 0.5 Tmm present in the cooler telescope of otherwise ideal COSY ring.

the data of Fig. 1 appear not to be consistent, which is evidenced by the rather large $\chi^2/\mathrm{ndf} = 17.65$.

During the 2$^{\mathrm{nd}}$ run, we would like to apply the pilot-bunch approach for the spin-tune feedback. Recording the spin tune of the unperturbed pilot bunch acts as a co-magnetometer during the EDM measurement. This alone constitutes a potentially crucial step to better understand the systematics of the EDM precursor experiment. The requested beam time shall be used primarily for the items described below:

1. It is obvious that the data set, shown in Fig. 1, based on the initial slope needs to be substantially enhanced. As stated in Sec. 2.3, also the shape of the elliptic paraboloid is not completely understood. In order to sort this out, more and better data are required, using moderately long cycles of about 400 s duration, and measurements of the initial slopes at 9 different RF phases.

2. In order to apply a different technique than the one applied in the 1$^{\mathrm{st}}$ run, we would like to determine the orientation of the spin-closed orbit vector $\vec{n}_s$ at the RF Wien filter by moving into a regime of the elliptic paraboloid, where the oscillation frequency of $p_y(t)$ can be directly observed. This entails mapping out a wider region of rotation angles of the solenoid (ξ^{Sol}) and of the RF Wien filter (ϕ^{WF}). For this type of measurement, longer cycles are needed, of typical duration of 1000 s, while the number of different RF phases at which the data shall be recorded, can in that case be smaller, *i.e.,* about 4.

3. As a third item, we list here that measurements 1. and 2. from above shall be carried out not only using the Siberian snake solenoid, but also the solenoid of the 2 MV electron cooler, residing in the opposite straight section than the other solenoid, shall be used. These measurements provide an independent determination of the orientation of the spin-closed orbit vector $\vec{n}_s$ at the RF Wien filter.

It should be implicitly clear that the 2$^{\mathrm{nd}}$ run will be the last one for the JEDI precursor EDM experiment on the deuteron. The JEDI collaboration would like to request beam

item	solenoid	# of pts	cycle	repeat	no. of phases	time
1.	Snake	5×5	400 s	5	9	$25 \cdot 400\,\text{s} \cdot 5 \cdot 9 \approx 5.2\,\text{d}$
1.	2 MV cooler	5×5	400 s	5	9	$25 \cdot 400\,\text{s} \cdot 5 \cdot 9 \approx 5.2\,\text{d}$
2.	Snake	5×5	1000 s	5	4	$25 \cdot 1000\,\text{s} \cdot 5 \cdot 4 \approx 5.8\,\text{d}$
2.	2 MV cooler	5×5	1000 s	5	4	$25 \cdot 1000\,\text{s} \cdot 5 \cdot 4 \approx 5.8\,\text{d}$
						total time $= 22\,\text{d}$

Table 1: Under perfect conditions, the required beam time for the 2$^{\text{nd}}$ run amounts to about 22 d.

time to collect a statistically and systematically meaningful data sample for the deuteron EDM measurement. In Table 1, we briefly summarize how the requested beam time shall be utilized. From this it follows that under perfect conditions, the time needed to obtain the desired goals of the 2$^{\text{nd}}$ run amounts to about 22 d. Allowing for a contingency of $\approx$ 50%, we arrive at a request of 35 d of beam time. Given the experience from the previous JEDI experiments, also for this experiment, a longer setup time is needed, and therefore **we would like to request for the 2$^{\text{nd}}$ deuteron EDM measurement with the RF Wien filter, 2 weeks of machine development time and 5 weeks of measurement time**, to be tentatively scheduled during the 1$^{\text{st}}$ quarter of 2021. It should be noted that we would like to combine the beam time for this 2$^{\text{nd}}$ precursor run (E 005.7) with the beam time requested for the JEPO commissioning experiment (E 002.8).

References

[1] T. E. Chupp, P. Fierlinger, M. J. Ramsey-Musolf, and J. T. Singh, "Electric dipole moments of atoms, molecules, nuclei, and particles," Rev. Mod. Phys. **91**, 015001 (2019), URL https://link.aps.org/doi/10.1103/RevModPhys.91.015001.

[2] J. Jaeckel, M. Lamont, and C. Vallée, "The quest for new physics with the Physics Beyond Colliders programme," Nature Phys. **16**, 393 (2020).

[3] F. Rathmann, A. Saleev, and N. N. Nikolaev, "The search for electric dipole moments of light ions in storage rings," J. Phys. Conf. Ser. **447**, 012011 (2013).

[4] W. M. Morse, Y. F. Orlov, and Y. K. Semertzidis, "rf wien filter in an electric dipole moment storage ring: The "partially frozen spin" effect," Phys. Rev. ST Accel. Beams **16**, 114001 (2013), URL http://link.aps.org/doi/10.1103/PhysRevSTAB.16.114001.

[5] F. Rathmann, N. N. Nikolaev, and J. Slim, "Spin dynamics investigations for the electric dipole moment experiment," Phys. Rev. Accel. Beams **23**, 024601 (2020), URL https://link.aps.org/doi/10.1103/PhysRevAccelBeams.23.024601.

[6] H. Ströher, "Search for electric dipole moments using storage rings (srEDM)," (2015), Advanced grant of the European Research Council, Proposal number: 694340, available from http://collaborations.fz-juelich.de/ikp/jedi/public_files/proposals/Proposal-SEP-210276270.pdf.

[7] F. Abusaif et al., "Storage Ring to Search for Electric Dipole Moments of Charged Particles - Feasibility Study," (2019), https://arxiv.org/abs/1912.07881.

[8] T. Fukuyama and A. J. Silenko, "Derivation of Generalized Thomas-Bargmann-Michel-Telegdi Equation for a Particle with Electric Dipole Moment," Int. J. Mod.

Phys. **A28**, 1350147 (2013), URL https://www.worldscientific.com/doi/abs/10.1142/S0217751X13501479.

[9] J. Slim, R. Gebel, D. Heberling, F. Hinder, D. Hölscher, A. Lehrach, B. Lorentz, S. Mey, A. Nass, F. Rathmann, et al., "Electromagnetic simulation and design of a novel waveguide rf wien filter for electric dipole moment measurements of protons and deuterons," Nuclear Instruments and Methods in Physics Research Section A: Accelerators, Spectrometers, Detectors and Associated Equipment **828**, 116 (2016), ISSN 0168-9002, URL http://www.sciencedirect.com/science/article/pii/S0168900216303710.

[10] J. Slim, A. Nass, F. Rathmann, and G. Tagliente, "An improved pilot bunch-based spin phase-lock feedback system for the measurement of the deuteron electric dipole moment," (2019), JEDI Proposal E 005.6, available from http://collaborations.fz-juelich.de/ikp/jedi/public_files/proposals/ProposalGatingRFWienFilter.pdf.

[11] B. Alberdi Esuain, Master's thesis, Faculty of Mathematics, Computer Science and Natural Sciences, RWTH Aachen University (2019), optimization of Injection in COSY, URL http://collaborations.fz-juelich.de/ikp/jedi/public_files/theses/main.pdf.

[12] Vermessungsbüro Stollenwerk & Burghof (2019), Transformationsparameter with uncertainties, communicated by M. Schmühl (IKP-4), available from http://collaborations.fz-juelich.de/ikp/jedi/apps/wiki/images/7/7a/Transformationsparameter_mitSTD_aktuell.xlsx.

[13] T. Wagner and J. Pretz (JEDI), in *10th International Particle Accelerator Conference* (2019), p. THPGW024, URL https://inspirehep.net/files/ab7144780a088ae11247ce78f7856b5c.

[14] T. Wagner, A. Nass, J. Pretz, F. Abusaif, A. Aggarwal, A. Andres, I. Bekman, N. Canale, I. Ciepal, G. Ciullo, et al., "Beam-based alignment at the cooler synchrotron cosy as a prerequisite for an electric dipole moment measurement," (2020), URL https://arxiv.org/pdf/2009.02058.pdf.

[15] D. Eversmann, V. Hejny, F. Hinder, A. Kacharava, J. Pretz, F. Rathmann, M. Rosenthal, F. Trinkel, S. Andrianov, W. Augustyniak, et al. (JEDI), "New method for a continuous determination of the spin tune in storage rings and implications for precision experiments," Phys. Rev. Lett. **115**, 094801 (2015), URL http://link.aps.org/doi/10.1103/PhysRevLett.115.094801.

[16] S. Park et al., "Axion-EDM: An Axion Search at COSY," (2018), JEDI proposal, available from http://collaborations.fz-juelich.de/ikp/jedi/public_files/proposals/Beam_time_request_E7andE8.pdf.

[17] G. Guidoboni, E. J. Stephenson, A. Wrońska, Z. Bagdasarian, J. Bsaisou, S. Chekmenev, G. Ciullo, S. Dymov, D. Eversmann, M. Gaisser, et al. (JEDI Collaboration), "Connection between zero chromaticity and long in-plane polarization lifetime in a magnetic storage ring," Phys. Rev. Accel. Beams **21**, 024201 (2018), URL https://link.aps.org/doi/10.1103/PhysRevAccelBeams.21.024201.

[18] F. Müller, Ph.D. thesis, Fakultät für Mathematik, Informatik und Naturwissenschaften der RWTH Aachen University (2019), URL http://collaborations.

fz-juelich.de/ikp/jedi/public_files/theses/thesis_fabian_mueller_final_version.pdf.

[19] J. Slim, A. Nass, F. Rathmann, H. Soltner, G. Tagliente, and D. Heberling, “The driving circuit of the waveguide RF Wien filter for the deuteron EDM precursor experiment at COSY,” JINST **15**, P03021 (2020), URL https://iopscience.iop.org/article/10.1088/1748-0221/15/03/P03021/pdf.

[20] J. Slim, F. Rathmann, A. Nass, H. Soltner, R. Gebel, J. Pretz, and D. Heberling, “Polynomial chaos expansion method as a tool to evaluate and quantify field homogeneities of a novel waveguide {RF} wien filter,” Nuclear Instruments and Methods in Physics Research Section A: Accelerators, Spectrometers, Detectors and Associated Equipment **859**, 52 (2017), ISSN 0168-9002, URL http://www.sciencedirect.com/science/article/pii/S0168900217303807.

[21] F. Abusaif, “Development of compact highly sensitive beam position monitors for storage rings,” Hyperfine Interactions **240**, 4 (2019), URL https://link.springer.com/article/10.1007/s10751-018-1543-x.

[22] G. Hashmi, M. Lehtonen, and A. Elhaffar, in *19th International Conference on Electricity Distribution, Vienna, 21-24 May* (2007), p. 0207, URL https://pdfs.semanticscholar.org/5b4f/8e18b04b24b81b7158e915fd32137dad26f4.pdf?_ga=2.41242722.1796073613.1599212894-42769671.1599212894.

[23] G. Robles, M. Shafiq, and J. Martínez-Tarifa, “Designing a rogowski coil with particle swarm optimization,” Proceedings **4**, 10 (2018), ISSN 2504-3900, URL http://dx.doi.org/10.3390/ecsa-5-05721.

[24] T. Orosz, Z. A. Tamus, and I. Vajda, in *2014 49th International Universities Power Engineering Conference (UPEC)* (2014), pp. 1–4, URL https://ieeexplore.ieee.org/stamp/stamp.jsp?tp=&arnumber=6934663.

[25] A. Saleev, N. N. Nikolaev, F. Rathmann, W. Augustyniak, Z. Bagdasarian, M. Bai, L. Barion, M. Berz, S. Chekmenev, G. Ciullo, et al. (JEDI), “Spin tune mapping as a novel tool to probe the spin dynamics in storage rings,” Phys. Rev. Accel. Beams **20**, 072801 (2017), URL https://link.aps.org/doi/10.1103/PhysRevAccelBeams.20.072801.

[26] A. Saleev, “Optimization of the alignment of magnetic elements using the spin tune response to three-steerer bumps,” (2019), JEDI Proposal, available from http://collaborations.fz-juelich.de/ikp/jedi/public_files/proposals/Optimization-alignments-vs-bumps_v1.pdf.

[27] M. Berz, “Computational aspects of optics design and simulation: Cosy infinity,” Nuclear Instruments and Methods in Physics Research Section A: Accelerators, Spectrometers, Detectors and Associated Equipment **298**, 473 (1990), ISSN 0168-9002, URL http://www.sciencedirect.com/science/article/pii/016890029090649Q.